Stimuli-responsive intelligent nanomaterials self-assembled from rigid flexible molecules

Abstract

Aqueous nanofibers constructed by self-assembly of small amphiphilic molecules are able to entangle with each other to form hydrogels that have a variety of applications including tissue engineering, and controlled drug delivery. The hydrogels are formed through physical cross-links in a random way of flexible nanofibers. Here we report that the self-assembled nanofibers with a nematic substructure are aligned into a nematic liquid crystal and spontaneously fixed in the aligned state to give rise to anisotropic gels. The liquid crystal gels are responsive to temperature variation by transformation into a fluid solution on cooling. Thus, the nanofiber solution can be mixed with cells at room temperature and transformed into gels to encapsulate the cells in a 3D environment upon heating to physiological temperatures. We found that the cells grow within the 3D networks without compromising cell viability, and subsequent cooling triggers the encapsulated cells to be released through a sol-gel transition. We anticipate that our smart nematic gels offer novel opportunities in many biological applications including tissue regeneration and drug delivery vehicles.

Molecular self-assembly into one-dimensional (1D) objects has been the subject of intense study as a means of creating intelligent materials and devices for nanotechnology.[1-3] One of the most ubiquitous 1D self-assembly in nature is cytoskeleton components such as actin filaments and microtubules which are responsible for resisting tension and maintaining cellular shape. The self-assembled nanofibers in aqueous solution become easily entangled with each other to form networks that are well suited as scaffolds for gelation of solvent molecules and 3D cell culture.[4-9] In contrast to polymer networks, these supramolecular gels can be easily disintegrated by changing their environments because their formation is completely

Report Documentation Page

Form Approved
OMB No. 0704-0188

1. REPORT DATE	2. REPORT TYPE	3. DATES COVERED
19 NOV 2010	**FInal**	**07-05-2009 to 18-06-2010**

4. TITLE AND SUBTITLE
Stimuli-responsive intelligent nanomaterials self-assembled from rigid flexible molecules

5a. CONTRACT NUMBER
FA23860914116

5b. GRANT NUMBER

5c. PROGRAM ELEMENT NUMBER

6. AUTHOR(S)
Myong Soo Lee

5d. PROJECT NUMBER

5e. TASK NUMBER

5f. WORK UNIT NUMBER

7. PERFORMING ORGANIZATION NAME(S) AND ADDRESS(ES)
Seoul National University,Seoul,Seoul,Korea,KR,151-747

8. PERFORMING ORGANIZATION REPORT NUMBER
N/A

9. SPONSORING/MONITORING AGENCY NAME(S) AND ADDRESS(ES)
AOARD, UNIT 45002, APO, AP, 96337-5002

10. SPONSOR/MONITOR'S ACRONYM(S)
AOARD

11. SPONSOR/MONITOR'S REPORT NUMBER(S)
AOARD-094116

12. DISTRIBUTION/AVAILABILITY STATEMENT
Approved for public release; distribution unlimited

13. SUPPLEMENTARY NOTES

14. ABSTRACT
Aqueous nanofibers constructed by self-assembly of small amphiphilic molecules are able to entangle with each other to form hydrogels that have a variety of applications including tissue engineering, and controlled drug delivery. The hydrogels are formed through physical cross-links in a random way of flexible nanofibers. Here we report that the self-assembled nanofibers with a nematic substructure are aligned into a nematic liquid crystal and spontaneously fixed in the aligned state to give rise to anisotropic gels. The liquid crystal gels are responsive to temperature variation by transformation into a fluid solution on cooling. Thus, the nanofiber solution can be mixed with cells at room temperature and transformed into gels to encapsulate the cells in a 3D environment upon heating to physiological temperatures. We found that the cells grow within the 3D networks without compromising cell viability, and subsequent cooling triggers the encapsulated cells to be released through a sol-gel transition. We anticipate that our smart nematic gels offer novel opportunities in many biological applications including tissue regeneration and drug delivery vehicles.

15. SUBJECT TERMS
nanostructures, nanomaterials, stimuli-responsive materials , advanced materials

16. SECURITY CLASSIFICATION OF:			17. LIMITATION OF ABSTRACT	18. NUMBER OF PAGES	19a. NAME OF RESPONSIBLE PERSON
a. REPORT	b. ABSTRACT	c. THIS PAGE			
unclassified	**unclassified**	**unclassified**	**Same as Report (SAR)**	**12**	

reversible. The dynamic nature of the aggregates allows them to adapt to the changes in their surroundings. This plays a crucial role in artificial extracellular matrix that mimics the *in vivo* cell and tissue growth situation.[10-13]

Another interesting aspect regarding artificial network structures is the possibility of implementing rapid responses to external triggers. Combination of the principles of 3D networks with responsive properties generates a new class of intelligent nanomaterials for the use of functional biomaterials and controlled drug delivery systems.[14-19] Small amphiphilic molecules based on responsive building blocks have been shown as useful molecular modules for the creation and stabilization of responsive hydrogels based on noncovalent interactions.[20-24] Typical examples include peptide amphiphiles based on elastin-like oligopeptides, poly(N-isopropyl acrylamide), and poly(ethylene oxide) chains that form nanofibers and subsequently, entangle with each other to form stimuli responsive hydrogels.[25,26] Introduction of such responsive segments into self-assembling block molecules not only enhances its solubility in water solvent but also endows the nanofibers with a responsive property due to thermally regulated dehydration.[27] Although numorous examples of stimuli-responsive gels have been reported, most of them are based on isotropic networks.[28,29] Herein, we report the formation of supramolecular nanofibers with a nematic substructure in aqueous solution that are aligned parallel to each other to form nematic networks (Figure 1).

Results and disscusion

The anisotropic opaque gel reversibly transforms into a transparent solution on cooling, as opposed to conventional gels. This responsive gel is derived from the self-assembly of laterally grafted rod amphiphiles that consist of a penta-*p*-phenylene rod and a laterally grafted dendritic oligoether chain through an imidazole linkage.[30,31] Aggregation behavior of the molecules was investigated in aqueous solution by using transmission electron microscopy (TEM). Molecule **1** based on a shorter di(ethylene oxide) chain showed to be insoluble in water, however, addition of MeOH induces self-assembled nanostructures. Figure 2a shows a micrograph obtained from a 0.01 wt% mixed solution (H_2O:MeOH=7:3 v/v) of **1** cast onto a TEM grid. The negatively stained sample with uranyl acetate shows the formation of tubules with uniform diameters of ~80 nm and interior of ~40 nm in diameter. The nanotubes appear as white periphery separated by a dark interior, characteristic of projection images of hollow tubules. The walls consist of multilayers with a primary spacing of ~4.5 nm. This dimension corresponds roughly to the laterally extended molecular length, suggesting that the rod segments within the domains are parallel to the layer planes within which the rod

segments are aligned parallel to each other to form in-plane nematic-like organization. Similar to the bulk organization of other laterally-grafted rod-coil molecules,[30,31] the tubules seem to stem from rolling-up of the initially-formed anisotropic layers along the rod direction.

We envisioned that an increment of the volume fraction of the dendritic flexible chain would enforce the layers to split along the rod direction into elongated fibers to reduce steric crowdings bewteen the larger dendritic chains.[32] Indeed, TEM image of **2** based on a longer tri(ethylene oxide) chain obtained from a 0.01 wt% aqueous solution shows the formation of nanofibers with a uniform diameter of ~8 nm and lengths of several micrometers (Figure 2b). This dimension of the diameter with large disrepancy to the molecular dimensions (~ 5.5 nm) suggests that the rod segments are directed prallel to the fiber axis within the aromatic core surrounded by hydrophilic dendritic chains. The formation of the elongated objects in bulk solution was further confirmed by dynamic light scattering (DLS) experiments in which the angular dependence of the apparent diffusion coefficient (D_{app}) is consistent with the value predicted for cylindrical aggregates.

To gain insight into the packing arrangements of the rod segments within the 1D aromatic domains, UV-Vis and fluorescence measurements were caried out with the aqueous solution (0.01 wt%) of **2** (Figure 2c). The absorption spectrum of the aqueous solution shows a broad transition with a maximum of 350 nm that is red-shifted relative to that observed in $CHCl_3$ solution. Notably, the fluorescence spectrum of the aqueous solution exhibits an enhanced strong emission compared to the $CHCl_3$ solution. Both red-shifted absorption and enhanced fluorescence intensity are characteristic of J-type aggregates of chromophores, suggesting that the rod segments are aligned with a nematic-like slipped arrangement within the 1D aromatic domains.[33,34] Based on this result together with the dimension of the fiber in diameter, the rod segments can be considered to be aligned parallel to each other along the fiber axis, giving rise to highly fluorescent nanofibers (Figure 1b). This is in significant contrast to conventional nanofibers based on conjugated rods that exhibit strong fluorescence quenching,[1] and implies how to construct light-emitting 1D nanostructures without fluorescent quenching.

The formation of nanofibers with oligoether dendritic exterior suggests that the aqueous solution would exhibit thermoresponsive behavior, because the degree of hydration of the ethylene oxide chains decreases with increasing temperture. As shown in Figure 3, the transparent nanofiber solutions at concentrations above 0.8 wt% undergo turbid gelation upon heating and the resulting gels appear to be strongly

birefringent. This appearance of birefringence is indicative of a transition between two states with different alignments of the nanofibers. The optical polarized micrograph of the gels exhibits a thread-like texture (Figure 3c), characteristic of a nematic liquid crystalline phase that rapidly transforms into isotropic liquid on cooling. The transition temperature decreases to 10 ^{o}C with increasing temperature up to 6.0 wt%. As shown in Figure 3e, dynamic viscoelasticity measurements of an aqueous solution (3 wt%) shows a frequency-independent storage modulus (G') of which the value is much larger than that of the loss modulus (G"), indicative of the formation of a nematic gel above the transition temperature.[35] The storage modulus measurements as a function of temperature for heating/cooling cycles indicate that the sol-gel transition is completely reversible with subsequent temperature cycles (Figure 3f). At 30 ^{o}C, the solution exists as a self-supporting gel (G'=120Pa). Cooling to 10 ^{o}C results in gel dissolution and low G' values consistent with a freely fluid solution that immediately recovers to the gel state upon subsequent heating.

TEM image of the gel dried on a carbon-coated copper grid reveals parallel alignments of the nanofibes at higher temperatures (Figure 3d), which demonstrates that the gel formation is attributed to the nematic alignments of the randomly oriented nanofibers. Consequently, heating the solution drives the fluid state to transform into anisotropic gels in which the elementary fibers are interconnected to each other to immobilize solvent molecules. This thermoresponsive solution behavior can be explained by considering entropically-driven dehydration of the oligoether chains, as the solution is heated.[36] This dehydration allows the exterior of the nanofibers to become more hydrophobic, thus resulting in enhanced hydrophobic interactions between adjacent nanofibers to form gels. Another interesting point to be noted is that the lyotropic liqid crystal forms at an unususally low concentration (0.8 wt%) of the rod segment. This unusual solution behavior seems to stem from the formation of the supramolecular nanofibers with a high persistent length imparted by a nematic substructure of the rod segments aligned along the fiber axis.

The spontaneous fixation of the nanofibers in the gel state at a physiological condition holds great promise as artificial 3D cell culture scaffolds that mimic the natural extracellular matrix.[12,37] In particular, the stiffness of the gels (120 Pa in storage modulus) is suitable to maintain mammalian cells in 3D environments for tissue regeneration applications.[38] As the first step towards this direction, we prepared C2C12 cell (myoblast, mouse muscle adherent cells) containing gels for 3D cell culture. After mixing C2C12 cells with the nanofiber solutions, the solution was heated to the gelation temperature to encapsulate the cells within the gel matrix (Figure 4a). These adherent

cells remain alive with encapsulation within the nematic gels for at least 5 days (Figure 4b), which indicates that the nematic gels are cytocompatible without compromising cell viability. Optical microscopy images of C2C12 for 2days indicate that the density of the cells increases to form cell colonies in the gel matrix (Figure 4c), as opposed to growing as a monolayer on tissue-culture plastic (2D) (see the Supporting Information). This result demonstrates that the cells can proliferate in the 3D gel systems and thus the gels effectively offer a 3D culture environment to C2C12 cells. Notably, we found that the encapsulated cells are released upon cooling to the tempreatures below the sol-gel transition. The ability of the gels to encapsulate and release cells remaining alive provides the potential for ex vivo cellular scaffolds.

Conclusions

In summary, we have been able to construct thermo-responsive nematic gels through the self-assembly of water soluble nanofibers with a nematic substructure. The nematic alignment of the armatic segments imparts the nanofibers to be highly fluorescent due to J-aggregates within the core of the nanofibers. These light-emitting nematic gels spontaneously transform into a transparent solution upon cooling. The sol-gel transition allows encapsulation and growth of myoblast cells inside the 3D networks at a physiological condition. Consequently, the gels guide C2C12 cells to be encapsulated, viable and raised in a 3D environment, and subsequent cooling triggers the encapsulated cells to be released through sol-gel transition. Liquid crystal gels containing cells may be aligned along the fiber direction in appropriate conditions to yield macroscopically aligned monodomains for directional cell growth.[28,39] In this regard, we anticipate that our anisotropic gels provide new opportunities to construct an artificial extracellular matrix for tissue engineering and regenerative medicine that require directed cell growth.

References

[1] Hoeben, F. J. M.; Jonkheijm, P.; Meijer, E. W.; Schenning, A. P. H. J. *Chem. Rev.* **2005,** *105***,** 1491-1546.

[2] Ryu, J.-H.; Hong, D.-J.; Lee, M. *Chem. Commun.* **2008**, 1043-1054.

[3] Palmer, L. C.; Stupp, S. I. *Acc. Chem. Res.* **2008**, *41*, 1674-1684.

[4] Ajayaghosh, A.; Praveen, V. K. *Acc. Chem. Res.* **2007**, *40*, 644-656.

[5] Kishida, T.; Fujita, N.; Sada, K.; Shinkai, S. *J. Am. Chem. Soc*. **2005**, *127*, 7298-7299.

[6] Lee, E.; Kim, J.-K.; Lee, M. *Angew. Chem. Int. Ed*. **2008**, *47*, 6375-6378.

[7] Hamley, I. W. *Angew. Chem. Int. Ed*. **2007**, *46*, 8128-8147.

[8] Cameral, F.; Ziessel, R.; Donnio, B.; Bourgogne, C.; Guillon, D.; Schmutz, M.; Iacovita, C.; Bucher, J.-P. *Angew. Chem. Int. Ed*. **2007**, *46*, 2659-2662.

[9] Kim, H.-J.; Lee, J.-H.; Lee M. *Angew. Chem. Int. Ed*. **2005**, *44*, 5810-5814.

[10] Deming, T. J. *Nat. Mater.* **2010**, *9*, 535-536.

[11] Silva, G. A.; Czeisler, C.; Niece, K. L.; Beniash, E.; Harrington, D. A.; Kessler, J. A.; Stupp, S. I. *Science* **2004**, *303*, 1352-1355.

[12] Cushing, M. C.; Anseth, K. S. *Science* **2007**, *316*, 1133-1134.

[13] Prestwich, G. D. *Acc. Chem. Res.* **2008**, *41*, 139-148.

[14] Petka, W. A.; Harden, J. L.; McGrath, K. P.; Wirtz, D.; Tirrell, D. A. *Science* **1998**, *281*, 389-392.

[15] Löewik, D. W. P. M.; Leunissen, E. H. P.; Van den Heuvel, M.; Hansen, M. B.; Van Hest, J. C. M. *Chem. Soc. Rev.* **2010**, *39*, 3394-3412.

[16] Bowerman, C. J.; Nilsson, B. L. *J. Am. Chem. Soc*. **2010**, *132*, 9526-9527.

[17] Cui, Z.; Lee, B. H.; Bernon, B. L. *Biomacromolecules* **2007**, *8*, 1280-1286.

[18] Motogawa, R.; Morishita, K.; Koizumi, S.; Nakahira, T.; Annaka, M. *Macromolecules* **2005**, *38*, 5748-5760.

[19] Grove, T. Z.; Osuji, C. O.; Forster, J. D.; Dufresne, E. R.; Regan, L. *J. Am. Chem. Soc.* **2010**, *132*, 14024-14026.

[20] Kloxin, A. M.; Kasko, A. M.; Salinas, C. N.; Anseth, K. S. *Science* **2009**, *324*, 59-

63.

[21] Zhao, X.; Pan, F.; Xu, H.; Yaseen, M.; Shan, H.; Hauser, C. A. E.; Zhang, S.; Lu, J. R. *Chem. Soc. Rev.* **2010**, *39*, 3480-3498.

[22] Balamurugan, S. S.; Bantchev, G. B.; Yang, Y.; McCarley, R. L. *Angew. Chem. Int. Ed*. **2005**, *44*, 4872-4876.

[23] Moon, K. S.; Kim, H.-J.; Lee, E.; Lee, M. *Angew. Chem. Int. Ed*. **2007**, *46*, 6807-6810.

[24] Pochan, D. J.; Schneider, J. P.; Kretsinger, J.; Ozbas, B.; Rajagopal, K.; Haines, L. *J. Am. Chem. Soc*. **2003**, *125*, 11802-11803.

[25] Nuhn, H.; Klok, H. A. *Biomacromolecules* **2008**, *9*,2755-2763.

[26] Börner, H. G.; Schlaad, H. *Soft Matter* **2007**, *3*, 394-408.

[27] Wright, E. R.; Contocello, V. P. *Adv. Drug Delivery Rev.* **2002**, *54*, 1057-1073.

[28] Zhang, S.; Greenfield, M. A.; Mata, A.; Palmer, L. C.; Bitton, R.; Mantei, J. R.; Aparicio, C.; De la Cruz, M. O.; Stupp, S. I. *Nat. Mater.* **2010**, *9*, 594-601.

[29] Aggeli, A.; Bell, M.; Carrick, L. M.; Fishwick, C. W. G.; Harding, R. H.; Mawer, P. J.; Radford, S. E.; Strong, A. E.; Boden, N. *J. Am. Chem. Soc*. **2003**, *125*, 9619-9628.

[30] Hong, D.-J.; Lee, E.; Jeong, H.; Lee, J.-K.; Zin, W.-C.; Nguyen, T. D.; Glotzer, S. C.; Lee, M. *Angew. Chem. Int. Ed*. **2009**, *48*, 1664-1668.

[31] Hong, D.-J.; Lee, E.; Choi, M.-G.; Lee, M. *Chem. Commun.* **2010**, *46*, 4896-4898.

[32] Lee, E.; Kim, J.-K.; Lee, M. *J. Am. Chem. Soc.* **2009**, *131*, 18242-18243.

[33] Mishra, A.; Ma, C.-Q.; Bäuerle, P. *Chem. Rev.*, **2009**, *109*, 1141-1276.

[34] Como, E. D.; Loi, M. A.; Murgia, M.; Zamboni, R.; Muccini, M. *J. Am. Chem. Soc*. **2006**, *128*, 4277-4281.

[35] Sugihara, S.; Kanaoka, S.; Aoshima, S. *Macromolecules* **2005**, *38*, 1919-1927.

[36] Dormidontova, E. E. *Macromolecules* **2002**, *35*, 987-1001.

[37] Lutolf, M. P.; Hubbell, J. A. *Nat. Biotech.* **2005**, *23*, 47-55.

[38] Kretsinger, J. K.; Haines, L. A.; Ozbas, B.; Pochan, D. J.; Schneider, J. P. *Biomaterials* **2005**, *26*, 5177-5186.

[39] Merzlyak, A.; Indrakanti, S.; Lee, S.-W. *Nano Lett.* **2009**, *9*, 846-852.

FIGURES

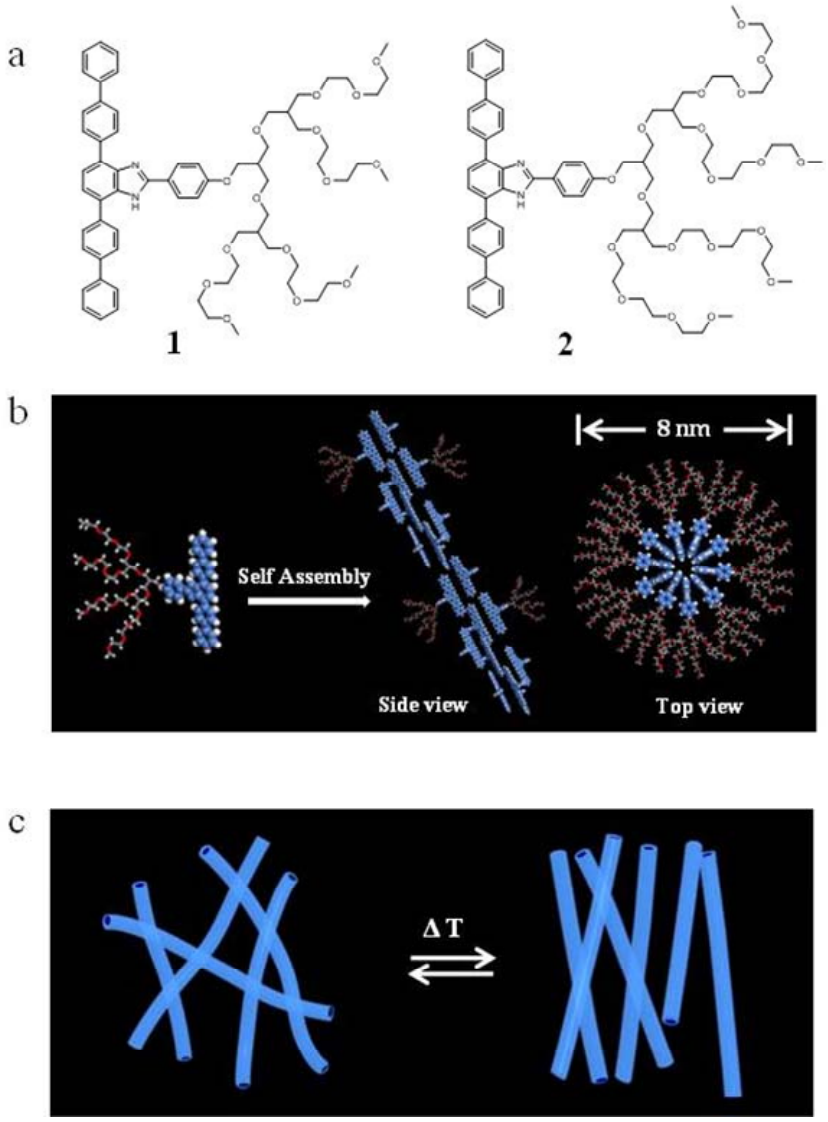

Figure 1 Molecular structure and self-assembly. a, Molecular structure of laterally grafted rod amphiphiles. **b,** Schematic representation of molecular packing arrangements in the nanofibers. **c,** Schematic representation of a reversible sol-gel phase transition of supramolecular nanofibers.

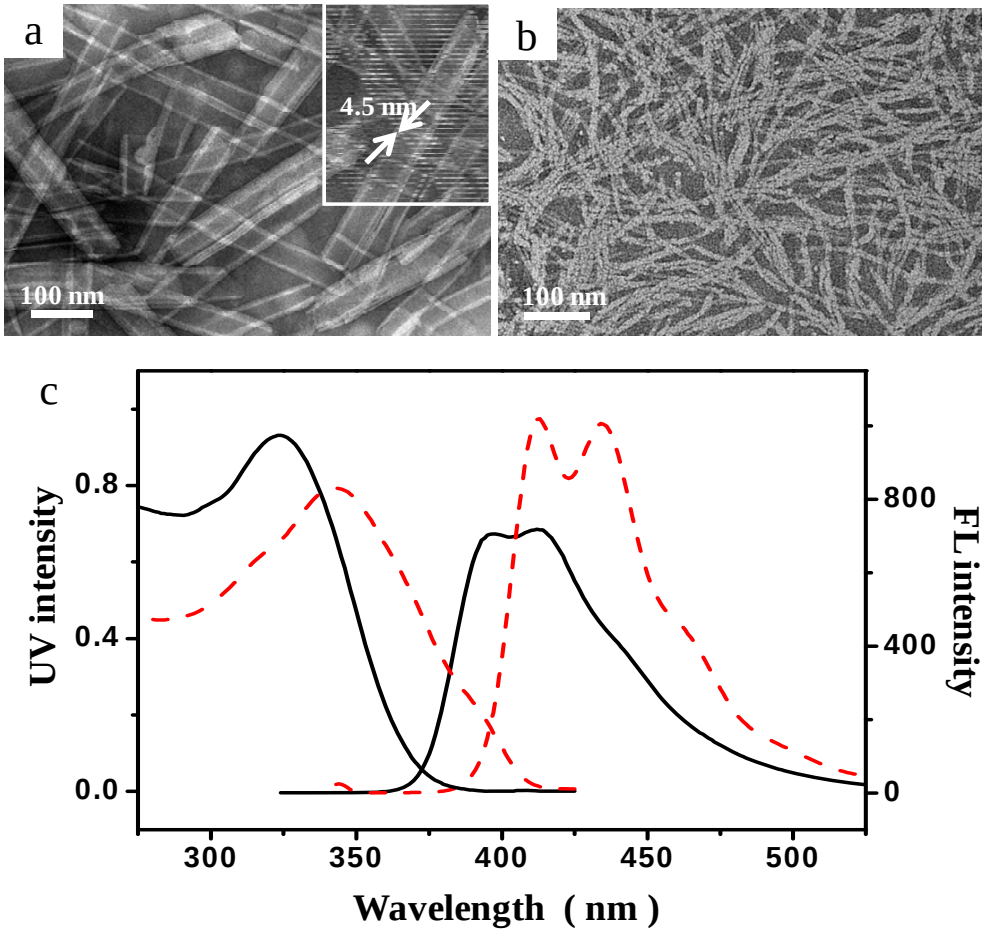

Figure 2 TEM images and optical characterizations. a, TEM image of **1** from 0.1 wt% mixed solution (H_2O : MeOH = 7 : 3 v/v). The inset is the high magnification image. **b,** TEM image of **2** from 0.1 wt% aqueous solution (stained with uranyl acetate). **c,** Absorption and emission spectra of 0.01 wt% of **2** in $CHCl_3$ (black and solid line) and aqueous solution (red and dashed line).

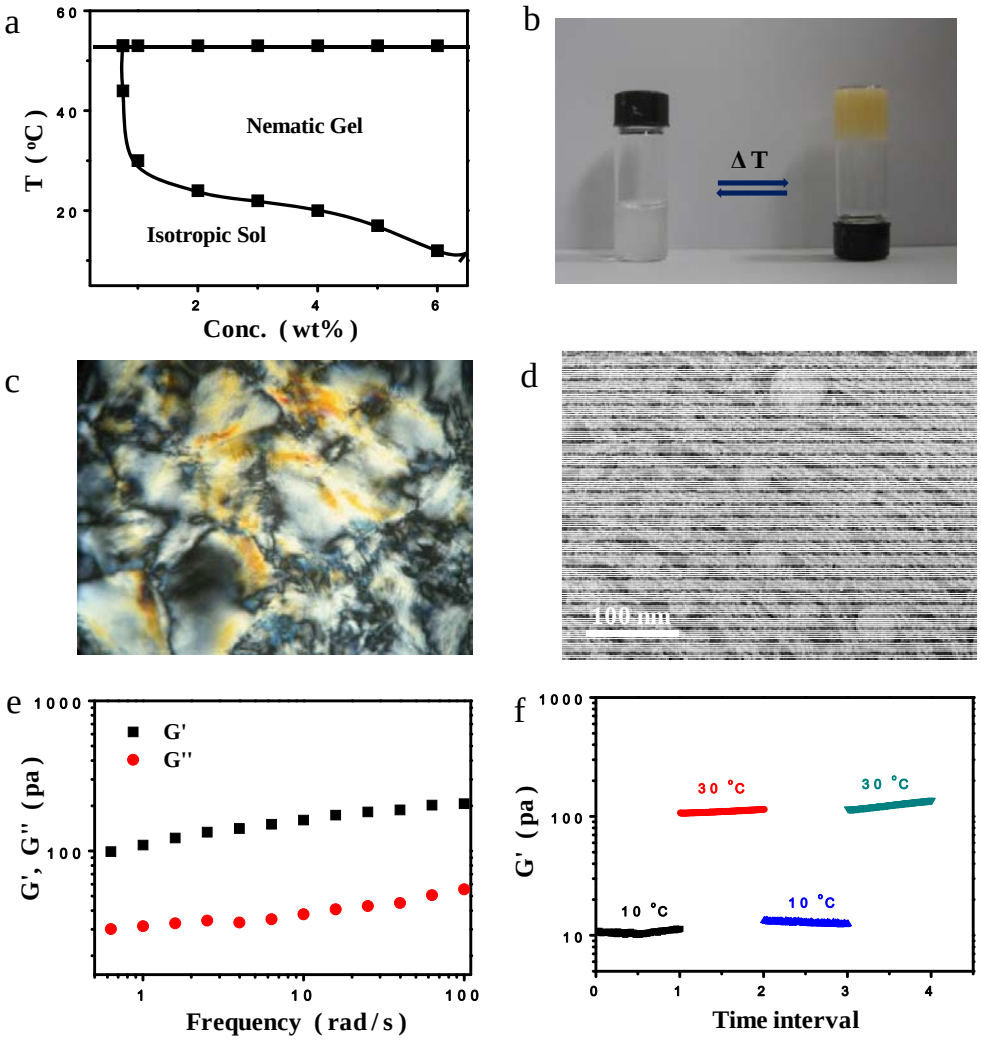

Figure 3 Sol-gel interconversion. a, Phase diagram plotted in terms of the concentration of **2** versus temperature. **b,** Optical image of reversible transformation from aqueous solution to nematic gel. **c,** A representative optical polarized micrograph of a nematic gel phase. **d,** TEM image of nematic gel of **2** with 1 wt% at 30 ^{o}C. **e,** G' and G" values of the nematic gels of **2** (3 wt% aqueous solution) on frequency sweep (from 0.1 to 100 rad / s). **f,** Temperature dependency of the storage modulus (G') for a 3 wt% aqueous preparation of **2** (data were collected at the 10 and 30 ^{o}C for 20 min time intervals).

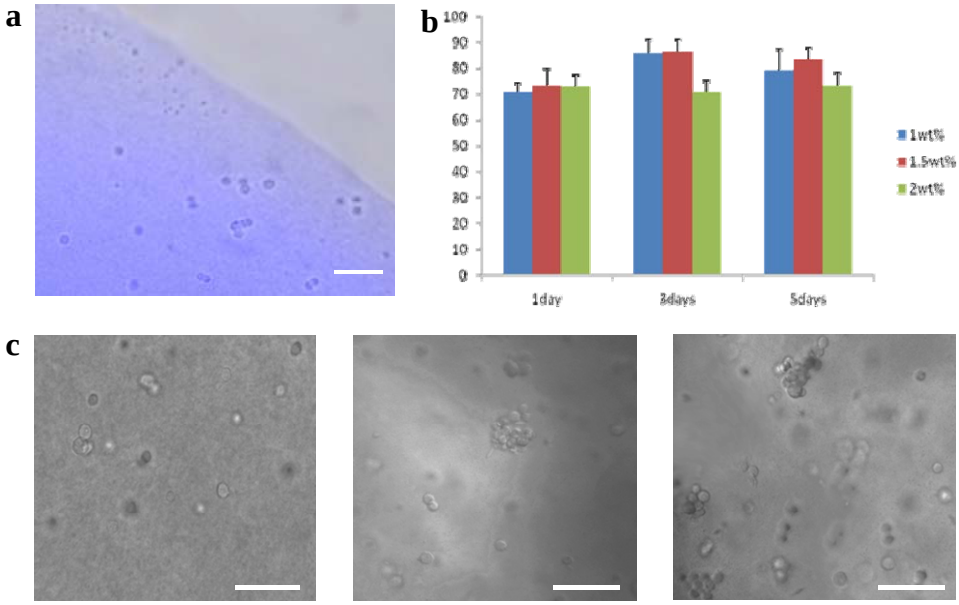

Figure 4 Encapsulation of myoblast cells in nanofiber gels. a, Optical image of C2C12 cells after 1day culture in nanofiber gel. DIC and blue fluorescence images were obtained at the same position of the cultured C2C12 cell. The blue region means nanofiber. **b,** The viability test of C2C12 cells using water soluble tetrazolium salt (WST) in various nanofiber gel concentration conditions for 5days. The Y axis means viability %. **c,** Optical images of C2C12 cells in nanofiber gel (Left: immediately after seeding, Middle: 1day, Right: 2days). The scale bars in all the images are 100 μm.

References published under AOARD Grant

[1] Kim, J.-K.; Lee, E.; Kim, M.-C.; Sim, E.; Lee, M. *J. Am. Chem. Soc*. **2009**, *131*, 17768-17770.

[2] Lim, Y.-b.; Lee, E.; Lee, M. *Macomol. Rapid Commun*. **2010**, *in press*.

[3] Kim, H.-J.; Kim, T.; Lee, M. *Acc. Chem. Res*. **2010**, *in press*.

[4] Huang, Z.; Lee, H.; Lee, E.; Kang, S.-K.; Nam, J.-M.; Lee, M. *Nat. Commun*. **2010**, *submitted*.